Multiple modes of RyR2 inhibition by flecainide

D. Mehra, M.S. Imtiaz, D.F. van Helden, B.C. Knollmann and D.R. Laver

Affiliations:

School of Biomedical Sciences and Pharmacy, University of Newcastle and Hunter Medical

Research Institute, Callaghan, NSW 2308, Australia; DM, MSI, DvH, DRL

Division of Clinical Pharmacology, Department of Medicine. Vanderbilt University School

of Medicine, Nashville, USA; BCK

Running Title: Flecainide inhibition of RyR2

To whom correspondence should be addressed:

Dr Derek Laver

School of Biomedical Sciences and Pharmacy,

University of Newcastle and Hunter Medical Research Institute,

Callaghan, NSW 2308, Australia

Phone: 61-2-4921-8732

FAX: 61-2-4921-9603

Email: Derek.Laver@newcastle.edu.au

31 pages text

1 table

9 figures

1 supplemental figure

 47 references

Abstract: 248 words

Introduction: 545 words

Discussion: 1417 words

Non-standard abbreviations: Catecholaminergic polymorphic ventricular tachycardia

(CPVT); cardiac ryanodine receptors (RyR2); sarcoplasmic reticulum (SR); calsequestrin

(CASQ2); cardiac voltage-dependent sodium channels (Nav1.5); (N -tris[hydroxymethyl]

methyl-2-aminoethanesulfonic acid (TES); (1,2-bis(o-aminophenoxy)ethane-N, N, N', N'-

tetraacetic acid (BAPTA); Hidden Markov Model (HMM)

ABSTRACT

Catecholaminergic polymorphic ventricular tachycardia (CPVT) causes sudden cardiac death due to mutations in cardiac ryanodine receptors (RyR2), calsequestrin or calmodulin. Flecainide, a Class I anti arrhythmic drug, inhibits Na^+ and RyR2 channels and prevents CPVT. The purpose of this study is to identify inhibitory mechanisms of flecainide on RyR2. RyR2 were isolated from sheep heart, incorporated into lipid bilayers and investigated by single channel recording under various activating conditions including the presence of cytoplasmic ATP (2 mM) and a range of cytoplasmic $[Ca^{2+}]$, $[Mg^{2+}]$, pH and [caffeine]. In Flecainide applied to either the cytoplasmic or luminal sides of the membrane inhibited RyR2 by two distinct modes: 1) a fast block consisting of brief substate and closed events with mean duration of ~ 1 ms, and 2) a slow block consisting of closed events with a mean duration of ~ 1 s. Both inhibition modes were alleviated by increasing cytoplasmic pH from 7.4 to 9.5 but were unaffected by luminal pH. The slow block was potentiated in RyR2 channels that had relatively low open probability whereas the fast block was unaffected by RyR2 activation. These results show that these two modes are independent mechanisms for RyR2 inhibition, both having a cytoplasmic site of action. The slow mode is a closed channel block whereas the fast mode blocks RyR2 in the open state. At diastolic cytoplasmic $[Ca^{2+}]$ (100 nM), flecainide possesses an additional inhibitory mechanism that reduces RyR2 burst duration. Hence, multiple modes of action underlie RyR2 inhibition by flecainide.

INTRODUCTION

In cardiac excitation-contraction coupling, the action potential depolarises the L-type Ca^{2+} channel leading to the Ca^{2+} release from the sarcoplasmic reticulum (SR) via RyR2 Ca^{2+} release channels located on the SR membrane (Nabauer et al., 1989). Following Ca^{2+} release, Ca^{2+} is sequestered into the SR via the SR Ca^{2+} ATPase or extruded from the cell by the Na/Ca exchanger (Dibb et al., 2007). The role of SR Ca^{2+} uptake and release (Ca^{2+} cycling) in maintaining the cardiac rhythm is highlighted by the arrhythmias associated with Ca^{2+} store overload. One such arrhythmia linked to the SR overload is Catecholaminergic Polymorphic Ventricular Tachycardia (CPVT) (Blayney and Lai, 2009). Mutations in RyR2 (George et al., 2003; Priori et al., 2001), calsequestrin (CASQ2) (Postma et al., 2002) or calmodulin (Nyegaard et al., 2012) can cause CPVT. These mutations increase RyR2 leak causing spontaneous Ca^{2+} release due to excessive diastolic Ca^{2+} release. This activates the Na/Ca exchanger in the plasmalemma that produces the inward depolarising current underlying the delayed after depolarisations leading to arrhythmias (Knollmann et al., 2006a; Knollmann et al., 2006b; Liu et al., 2006).

Flecainide is an orally administered potent anti-arrhythmic agent that blocks cardiac sodium channels (Nav1.5) in a time and voltage-dependent manner to reduce the maximum upstroke velocity of the action potential (Borchard and Boisten, 1982; Campbell and Vaughan Williams, 1983; Kojima et al., 1989). The kinetics of flecainide block of Nav1.5 has been extensively studied (Anno and Hondeghem, 1990; Grant et al., 2000; Liu et al., 2002; Nagatomo et al., 2000; Nitta et al., 1992). It has a relatively high affinity for Nav1.5 channels in their open and inactivated states (Grant et al., 2000; Liu et al., 2002) compared to their closed state. The recent discoveries that flecainide also blocks RyR2 channels, supressed Ca^{2+} waves in CASQ2$^{-/-}$ cardiomyocytes and prevented CPVT in mice and humans (Watanabe et al., 2009) suggests that RyR2 block may contribute to anti-arrhythmic drug efficacy against

Ca^{2+}-triggered arrhythmias. This was demonstrated again more recently by the use of RyR2 block by carvedilol and its derivatives which prevented stress-induced ventricular tachyarrhythmias in RyR2-mutant mice (Zhou et al., 2011). However, previous attempts to employ RyR2 inhibitors to reverse effects of RyR2 mutations have not been successful in preventing arrhythmia (reviewed by McCauley and Wehrens, 2011; Watanabe and Knollmann, 2011). For example, the dual Na^+ and RyR2 antagonist, tetracaine did not suppress the Ca^{2+} waves in CASQ2$^{-/-}$ myocytes upon prolonged exposure (Hilliard et al., 2010; Watanabe et al., 2009). Thus, it appears that it is not RyR2 block *per se* that is important in preventing Ca^{2+} overload arrhythmias. Therefore, there is a need to understand mechanisms for pharmacological inhibition of RyR2 by flecainide. Although the flecainide dose-response for RyR2 inhibition has been measured (Watanabe et al., 2009), no detailed study has been done to examine the action of this drug on the channel and how it depends on RyR2 activation state.

Here we use single channel recording of RyR2 from sheep to develop a model for flecainide inhibition, which will provide an understanding of the action of the drug in cardiac muscle. The work reported here extends a previous finding that flecainide is an open channel blocker (Hilliard et al., 2010). We now identify multiple flecainide inhibitory mechanisms that contribute to flecainide block of RyR2.

MATERIALS AND METHODS

Single-Channel Measurements

SR vesicles containing RyR2 were isolated from sheep hearts and incorporated in artificial bilayer membranes as previously described (Laver et al., 1995). Briefly, lipid bilayers were formed across an aperture with diameter 150-250 mm of a delrin cup using a lipid mixture of phosphatidylethanolamine and phosphatidylcholine (8:2 wt/wt, Avanti Polar Lipids) in n-decane (50 mg/ml, ICN Biomedicals). During the SR vesicle fusion period, the *cis* (cytoplasmic) and chamber contained 250 mM Cs^+ (230 mM $CsCH_3O_3S$, 20 mM CsCl) + 1.0 mM $CaCl_2$ and the *trans* (luminal) chamber contained 50 mM Cs^+ (30 mM $CsCH_3O_3S$, 20 mM CsCl) + 0.1 mM $CaCl_2$. When ion channels were detected in the bilayer, the trans Cs^+ was raised to 250 mM by aliquot addition of 4 M $CsCH_3O_3S$. During experiments, the composition of the *cis* solution was altered by a perfusion system and the *trans* solution was altered by aliquot additions. The local perfusion (O'Neill et al., 2003) allowed exposure of single RyR2 to multiple drug concentrations applied in random sequence within ~ 3s.

Chemicals

All solutions were pH buffered using 10 mM TES (N -tris[hydroxymethyl] methyl-2-aminoethanesulfonic acid; ICN Biomedicals), and titrated to pH 7.4 using CsOH (ICN Biomedicals). A Ca^{2+} electrode (Radiometer) was used in our experiments to determine the purity of Ca^{2+} buffers and Ca^{2+} stock solutions as well as free $[Ca^{2+}]$ > 100 nM. Free Ca^{2+} was titrated with $CaCl_2$ and buffered using 4.5 mM BAPTA (1,2-bis(o-aminophenoxy)ethane- N , N , N ' , N ' - tetraacetic acid; obtained from Invitrogen; free $[Ca^{2+}]$ < 1 μM) or dibromo BAPTA (up to 2 mM; free $[Ca^{2+}]$ between 1-10 μM). Because all solutions applied in cis bath contained ATP (ATP chelates Ca^{2+} and Mg^{2+}), free levels of Mg^{2+} (added as $MgCl_2$) were calculated using estimates of ATP purity and effective Mg^{2+}

binding constants that were determined previously under our experimental conditions (Laver et al., 2004). The cesium salts were obtained from Aldrich chemical Company. $CaCl_2$ and $MgCl_2$ were obtained from BDH Chemicals. Caffeine and flecainide was obtained from Sigma (St Louise, USA) and were prepared as stock solutions in milliQ water.

Data Acquisition and Analysis

Experiments were carried out at room temperature (23 ± 2° C). Electric potentials expressed using standard physiological convention (*i.e.* cytoplasm relative to SR lumen at virtual ground). Control of the bilayer potential and recording of unitary currents was done using either an Axopatch 200B amplifier (Axon Instruments Pty, Ltd) or a Bilayer Clamp-525C (Warner Instruments). Channel currents were digitized at 50 kHz and low pass filtered at 5 kHz. Before analysis the current signal was redigitized at 5-10 kHz and low pass-filtered at 1-3 kHz. Single channel parameters, open probability, mean open time and mean closed time, were measured using a threshold discriminator at 50% of channel amplitude (Channel2 software by P.W. Gage and M. Smith, Australian National University, Canberra). Channel substate analysis was carried out using the Hidden Markov Model (HMM) (Chung et al., 1990). The algorithm calculated the idealised, multilevel, current time course (*i.e.* background noise subtracted) and the transition probability matrix from the raw signal using maximum likelihood criteria.

Individual readings of open probability, mean open time and closed times were derived from 30-60 s of RyR2 recording. Dwell-time histograms were compiled from 10^3-10^4 opening events. Hill equations were fitted to the dose-response data by the method of least squares. Average data are given as mean $\pm$ SEM. The significance multi-group comparisons are made using Anova ($p < 0.01$). The significance of the difference between pairs of control and test values was tested using Student's t-test (* $p < 0.05$ and ** $p < 0.01$).

RESULTS

General observations

RyR2 were near maximally activated (P_o = 0.98 ± 0.02) by cytoplasmic Ca^{2+} (100 μM) in the presence of 2 mM ATP. Addition of flecainide to the cytoplasmic bath (membrane potential + 40 mV) induced two modes of RyR2 inhibition that were associated with channel closures on the millisecond and second timescales (fast and slow modes, respectively; Figure 1A). The millisecond events represent transitions to a substate that are analysed in detail later (Figures 7 & 8). Our initial threshold analysis of channel gating lumped the substates together with complete channel closures.

Flecainide exhibited similar inhibiting kinetics when applied to the luminal side of the bilayer albeit with a higher IC_{50} (Figure 1B and Figure 1C, *c.f.* ○-cytosolic and ●-luminal). The IC_{50} for flecainide was strongly dependent on the ionic conditions (Figure 1C, Table 1). Reducing the cytosolic ionic strength from 250 mM to 150 mM caused a 5-fold decrease in the IC_{50} (Figure 1C *c.f.* △ and ◇), decreasing cytosolic free $[Ca^{2+}]$ from 100 μM to 100 nM also caused a 5-fold decrease (*c.f.* ○ and □) and adding 1 mM free Mg^{2+} to the cytosol caused a 3-fold decrease in the IC_{50} (*c.f.* ○ and △). The flecainide IC_{50}'s were also strongly dependent on membrane potential (Figure 1D). IC_{50} for cytoplasmic and luminal applications of flecainide had similar slopes on logarithmic plots of IC_{50} versus bilayer voltage, decreasing by factors of 3.2 ± 0.2 (*cyt;* ○) and 3.6 ± 0.5 (*lum;* ●) for each 25 mV depolarisation. The Hill coefficients derived from fitting the data ranged from 0.6 to 2 (Table 1). The higher than unity values for some the Hill coefficients indicate a multiple binding-site mechanism for flecainide inhibition.

Fast and slow modes of flecainide block at systolic [Ca^{2+}]

Since the potency of flecainide depended on the ionic conditions we aimed to determine if this was a property of one, or both modes of block. During Ca^{2+} release during systole, the [Ca^{2+}] in the dyad cleft reaches 100 μM (Cannell and Soeller, 1997). In the presence of 100 μM cytoplasmic Ca^{2+} (2 mM ATP), addition of 50 μM flecainide to the cytosol induced fast inhibition with very few long closures (*i.e.* minimal slow block; Figure 2A, middle trace) whereas long closures became much more apparent when 50 μM flecainide and 1 mM Mg^{2+} were added to the cytoplasmic bath (bottom trace). Mg^{2+} did not induce these long closures in the absence of flecainide (top trace). Addition of very high [Ca^{2+}] (*i.e.* 0.4 mM & 1.6 mM) in the absence of Mg^{2+} to the cytoplasmic bath also increased the frequency of long channel closures (Figure 2B). Thus it appears that the potency of the slow mode of flecainide block is highly sensitive to the presence of divalent cations on the cytoplasmic side of the channel.

These effects of divalent ionic conditions on the kinetics of flecainide block were quantified by compiling frequency histograms of open and closed times from single channel recordings (Figure 2C-E). Histograms were displayed using the log-bin method of (Sigworth and Sine, 1987), where individual exponential components appear as separate peaks centred on their time constant value. In these plots, the probability/frequency values are represented by their square roots because this provides uniform statistical scatter over the full range of times. Closed dwell-time histograms are presented as frequency of occurrence $F_c(t)$ of closed durations (*t*) rather than their probability, $P_c(t)$, ($F_c(t) = P_c(t)/\tau_o$, where τ_o is the mean open time) in order to give a better indication of the total closing rates for each mode of block.

Open dwell-time probability histograms exhibited one or two exponential decays with an overall mean open duration of ~100 ms in the absence of flecainide. Flecainide applied to either the cytoplasmic (Figure 2E) or luminal solutions (Supplemental Figure 1) shifted the

probability distributions to shorter times. The mean open duration, τ_o, varied as the inverse of flecainide concentration as shown in Figure 2F.

RyR2 closed dwell-time frequency distributions exhibited two features in the absence of flecainide (with 1 mM cytoplasmic Mg^{2+}); an exponential decay with time constant of 3 ms which is characteristic of Mg^{2+} inhibition (Figure 2C $\square$, see arrow labelled τ_{Mg}) plus the tail of a partially resolved peak with sub-millisecond time constant. Addition of 50 μM cytoplasmic flecainide introduced two exponentials in the closed time distributions with time constants of ~1 ms (fast mode) and ~1 s (slow mode) as seen in Figure 2C (O, see arrows labelled τ_F and τ_S, associated with fast and slow modes, respectively). In the absence of Mg^{2+}, (Figure 2C ●), the peak amplitude associated with the slow time constant was markedly reduced while the peak associated with the fast time constant was relatively unaffected. A similar effect was seen when 500 μM flecainide was added to the luminal bath (Supplemental Figure 1). Figure 2B and D show that increasing cytoplasmic Ca^{2+} in the mM range had a similar effect on flecainide inhibition as Mg^{2+}. Thus only slow mode of flecainide block is sensitive to the divalent ionic conditions.

Fast and slow modes of flecainide block at diastolic [Ca^{2+}]

We also analysed flecainide block at diastolic levels of cytoplasmic Ca^{2+} (0.1 μM and 2 mM ATP) to see if it shared the same mechanisms as seen at systolic [Ca^{2+}] (Figure 3). At these sub-activating levels of Ca^{2+}, RyR2 had a P_o = 0.14 ± 0.04 and mean open and closed times of ~20 and ~400 ms, respectively (Figure 3A, top trace). Dwell time histograms of closed events (Figure 3C, ●) exhibit two peaks centred at 0.2 and 200 ms. Addition of 50 μM flecainide to the cytoplasmic bath (Figure 3A, bottom trace); 1) increased the long time constant of closed times (τ_S, Figure 3E, ●), 2) caused a fast mode of block with a time constant, τ_F= 0.83 ± 0.08 (n=6) which did not vary with [flecainide] over the range 10-50 μM

(not shown) and 3) decreased the mean open time (τ_o, Figure 3F, ●). The fast closures caused the conversion of channel long-lasting openings present under control conditions to bursts of openings. Flecainide decreased the duration of these bursts from 36 ms down to 12 ms at 50 μM with an IC_{50} of 15 μM.

The effect of flecainide on τ_o and τ_F is similar to that seen in systolic $[Ca^{2+}]$ suggesting that the fast mode of block is the same in systole and diastole. However, the [flecainide]-dependencies of τ_S associated with the slow mode were different in systolic and diastolic $[Ca^{2+}]$ (Figure 3E, *c.f.,* dashed line and ●), the latter showing a positive [flecainide]-dependence. This could be explained by Ca^{2+} affecting the reaction rates of the slow mechanism and/or an apparent lengthening of closed events due to the superposition of slow mode closures and the long deactivated states of the channel that occur at sub-activating $[Ca^{2+}]$. Distinguishing these possibilities requires a direct measurement of the duration of individual slow mode blocked events, which is not possible when they are masked by these deactivated RyR2 closures.

To more directly measure the duration of slow mode block, we eliminated the masking by the RyR2 deactivated states by adding 5 mM caffeine to the cytoplasmic bath to increase the channel activation at 0.1 μM Ca^{2+} (Figure 3B, top trace). Addition of 50 μM flecainide under these conditions induced short and long closures of the channel (bottom trace) with closed time histograms shown in Figure 3D. The time constant, τ_S, was similar to that in the absence of caffeine (Figure 3E) but different to that at high Ca^{2+} concentrations (Figure 3E, dashed line) suggesting that a differences in the reaction rates contribute the different time constants of the slow mode of block at diastolic and systolic $[Ca^{2+}]$.

Slow mode of flecainide block is specific for RyR2 closed states

Figure 4 summarises the on- and off-rates for flecainide block by fast and slow modes under different channel activating conditions. The rates were derived from dwell-time histograms as described in the caption to Figure 4. The on-rate of the slow blocking mode was markedly reduced under conditions where RyR2 are strongly activated by cytoplasmic caffeine and/or Ca^{2+} compared to RyR2 at sub-activating $[Ca^{2+}]$ (Figure 4A, 0.1 µM Ca^{2+}) or where RyR2 are subjected to Ca^{2+} or Mg^{2+} inhibition (Figure 4A, 1 mM Ca^{2+} or Mg^{2+}). This suggests that the slow mode of block has a preference for the inactive RyR2 channel. The rates associated with the fast mode (Figure 4B) had a relatively weak dependence on the activating conditions compared to those for the slow mode. Nonetheless, the fast mode off-rate was 2-3 fold lower at 100 µM - 1 mM cytoplasmic $[Ca^{2+}]$ than at 0.1 µM while caffeine had only a minor effect on the fast off-rate.

We examined the hypothesis that RyR2 can only enter the slow mode of block via the closed/inactive state of the channel as depicted by the scheme in Figure 5A. According to this scheme, the on-rate increases proportionally with RyR2 closed probability (P_c). Hence, looking for a correlation between the flecainide slow on-rate and RyR2 closed probability in the same channel will test this hypothesis. We employed the well-known observation that RyR2 can exhibit substantial variations in open probability (modal gating) under steady activating conditions and that there are also channel-to-channel variations in activity. In this analysis, P_c was measured within the bursts of channel activity that occurred between the slow-mode blocked events. Flecainide on-rate exhibited a strong positive correlation with P_c under a range of activating conditions (Figure 5B). Moreover, the correlations were similar for all activating conditions except for cytoplasmic solutions containing 1 mM Ca^{2+} or Mg^{2+} that exhibited 2-fold higher on-rates. Thus, channels with low P_c gating modes also had low

on-rates and this accounts for nearly all of the dependence of the slow mode potency on the RyR2 activating conditions seen in Figure 4.

The proposed scheme is also consistent with the [flecainide]-dependencies of slow mode rates in Figure 5C where the on-rate for slow inhibition increased proportionally with flecainide concentration and the off-rate showed no significant dependence on concentration. The scheme is also consistent with [Mg^{2+}]-dependence of the rate *constants* for the slow mode (k_{Son} and k_{Soff}, Figure 5D) where it can be seen that k_{Son} and k_{Soff} did not show any dependence on [Mg^{2+}], thus confirming that these can be considered as constants describing the interaction of Mg^{2+} and flecainide on RyR2.

Effect of pH on flecainide inhibition

Flecainide is a monovalent cation at neutral pH with a positive charge on its amide group (pKa = 9.2) (Liu et al., 2003). At pH 7.4, 99% of the molecules are in the charged, protonated form whereas at pH 9.5, this fraction reduced to 40%. In order to know which form of flecainide is responsible for RyR2 inhibition we compare the rates of fast and slow modes flecainide inhibition at pH 7.4 and 9.5 as shown in Figure 6. The recordings in Figure 6A and B show that raising cytoplasmic pH from 7.4 to 9.5 markedly decreased the inhibition caused by 50 μM flecainide. This is shown for both the fast mode in Figure 6A (in the absence of Mg^{2+}) and for the slow mode in Figure 6B where 1 mM Mg^{2+} is present. Dwell-time histograms (Figures 6C & D) demonstrate that raising cytoplasmic pH from 7.4 to 9.5 attenuates the frequency of both short and long exponential components of the flecainide-induced closures. This occurred via a 6-fold reduction in the on-rate constant of slow mode (Figure 6E) and a 2-fold reduction in the fast mode (Figure 6F). The loss of potency at high pH indicates that the cationic form of flecainide mediates the bulk of slow and fast modes of block.

The relative effects of cytoplasmic and luminal pH on flecainide block were used to gain clues about the side (*i.e. cis* or *trans*) of action of flecainide on the RyR2. This is difficult to determine from flecainide alone because it appears to readily cross the bilayer. It is apparent from Figure 6E and F that the on-rates of slow and fast block for flecainide applied from cytoplasmic side were sensitive to cytoplasmic pH and not luminal pH. Moreover, increasing cytoplasmic pH could attenuate fast mode block by flecainide applied from the luminal side (Figure 6G). Together these results indicate that flecainide only has access to its site of action from the cytoplasmic side.

Substate block by flecainide fast mode

Single channel recording of the fast mode of block at +60 mV in the presence of 100 μM cytoplasmic Ca^{2+} and 2 mM ATP revealed that it was due to flecainide-induced transitions from the RyR2 open state to a conductance substate and flecainide induced transitions from the substate to the closed state (Figure 7A). Substate current level did not depend on flecainide concentration. The current/voltage relationships (Figure 7B) indicates a slope-conductance of 87 ± 5 pS for the substate and 525 ± 10 pS for the open state which was identical to that of the open state in the absence of flecainide.

We tested the hypothesis that the substate was due to the binding of a single flecainide molecule to the RyR2 and that the brief closures were due to the binding of 2 molecules as shown by the scheme in Figure 7C. The scheme predicts that transition rates from open state to substate and from substate to closed state are proportional to flecainide concentration whereas the corresponding reverse transition rates are concentration independent. The concentration-dependencies of rates shown in Figure 7D show that indeed this is the case. The transition rates for the fast inhibition were calculated using the HMM algorithm (Methods).

Voltage-dependence of flecainide inhibition

The voltage-dependence of the flecainide rate constants may provide clues to the location of its binding sites on the RyR2 molecule within the trans-membrane electric field. The flecainide slow-mode on-rate constant was strongly voltage-dependent whereas the off-rate constant had no voltage-dependence (Figure 8A). For the fast mode, the flecainide rate-constants were all voltage-dependant (Figure 8B). Transitions between open and substates (Figure 8B, circles) were relatively easy to resolve above the signal noise and therefore their rates could be observed over a wider voltage range than transitions between the substate and closed states. Increasing the bilayer potential difference from -20 to +80 mV increased the flecainide on-rate constant (●) by 20-fold and decreased the off-rate constant (○) by 5-fold. The voltage-dependence of the rate constants for transitions between the substate and closed states (Figure 8B, triangles) paralleled those of the open state and substate transitions albeit with 4-fold slower on-rate and 2-fold faster off-rate constants.

The Woodhull model of voltage-dependent ion block (Woodhull, 1973) attributes the voltage-dependence of each binding constant to the voltage-dependence of the electrostatic potential of the flecainide cation in the channel. According to this model, the voltage-dependence of the flecainide rate constants are related to the ionic charge of flecainide (z=1) and the relative positions of the flecainide binding sites (δ) and energy barriers (δ_b) in the trans-membrane electric field by:

$$k_{on} = k_{on}(0).\exp(\delta_b zFV/RT) \text{ and } k_{off} = k_{off}(0).\exp((\delta_b - \delta)zFV/RT)$$

where V is the bilayer potential, $k_{on}(0)$ and $k_{off}(0)$ are the binding constants at zero volts and F,R and T have their usual meanings. Values of δ are derived from the slopes of the log-linear plots shown in Figure 8. For cytoplasmic flecainide, $\delta = 0$ would indicate a location on the cytoplasmic side of the membrane and δ=1, the luminal side. For the slow inhibition, the

voltage-dependence of the ratio k_{Son}/k_{Soff} gives a value of $\delta = 1.15 \pm 0.14$ suggesting a binding

site for the slow mode that is much closer to the luminal bath potential than the cytoplasmic

bath. For the fast mode of flecainide block, the voltage-dependencies of the rates constant

were not readily interpreted within the framework of the Woodhull model because the slopes

of the voltage-dependencies varied over the experimental voltage range (δ ranged from 0 to

1.4 ± 0.4) and so did not give a unique value for δ.

$[Cs^+]$-dependence of flecainide inhibition

We measured the effect of reducing $[Cs^+]$ from 250 mM to 150 mM in order to match the

physiological ionic strength of the cytoplasm and found that the IC_{50} for flecainide block was

reduced ~5-fold (Figure 1C). In Figure 9 we examined the effect of this change in $[Cs^+]$ on

rate constants for fast and slow modes of flecainide block. The rate constants for fast

inhibition were insensitive to $[Cs^+]$ but reducing $[Cs^+]$ from 250 mM to 150 mM caused a

2.5-fold decrease in the off-rate constant for the slow mode. However, the change in off-rate

constant would account for only half (2.5-fold) of the decrease in the IC_{50} seen in Figure 1C.

An additional contribution to effect of $[Cs^+]$ on the IC_{50} may arise from the reduced channel

P_o in 150 mM $[Cs^+]$ (0.75 in 250 mM reducing to 0.37 in 150 mM, see $P_o max$ in Table 1),

leading to an increase in the on-rate for the closed state block as shown in Figure 5A and B.

Therefore, the increased potency of flecainide at lower $[Cs^+]$ is likely to be due to both a

reduction in the off-rate for the closed state, slow block and an increase in the closed state

probability of the channel.

DISCUSSION

This study presents a detailed analysis of the kinetics of RyR2 inhibition by flecainide and its dependence on the activation state of the channel and the overall scheme derived for inhibition is shown in Figure 10. We identify two modes of action of flecainide (fast and slow) are responsible for the RyR2 block previously reported by (Watanabe et al., 2009). The two modes of block are clearly distinguished at systolic cytoplasmic $[Ca^{2+}]$. The flecainide fast block is evident as relatively frequent transitions (~1 kHz) between the channel open state and a conductance substate and between that substate and the closed state. The kinetics of fast block (Figure 7C) follows the same scheme as block of RyR2 by quinidine and cocaine (Tsushima et al., 1996; Tsushima et al., 2002) where the substates correspond to periods when one drug molecule is bound to the RyR2 and that full closures occur when two molecules are bound. The on- and off-rates for fast block were insensitive to the open state of the channel. The flecainide slow block is seen as less frequent transitions (~ 1 Hz) between the open and closed states of the channel, which have not been previously reported. The kinetics of slow block is consistent with a scheme (Figure 5A) where block occurs from the RyR2 closed state and where flecainide induced long closures represent periods where a single flecainide molecule is bound to the RyR2. The pH-dependencies of fast and slow flecainide block (Figure 6) indicate that these blocking modes are mediated predominantly by the protonated, cation form of flecainide.

The kinetics of flecainide block at diastolic cytoplasmic $[Ca^{2+}]$ is different to that seen under systolic $[Ca^{2+}]$ (*c.f.* Figures 2 and 3). The time-constants for the dwell-times associated with the fast mode of inhibition are similar in diastolic and systolic conditions suggesting that the fast mode operates in a similar way under both systolic and diastolic conditions. However, the kinetics of the slow mode measured in systolic $[Ca^{2+}]$ do not account for the properties of the slow mode inhibition at diastolic $[Ca^{2+}]$ in two respects: 1) the [flecainide]-dependencies

of long closed times (τ_S) are very different (Figure 3E) and 2) the on-rate constant for slow

block in systolic [Ca^{2+}] (k_{Son} = 0.05 μMs^{-1}; Figure 8A at +40mV) is 20-fold too slow to

account for the reduction in burst duration (36 ms to 12 ms) brought about by 50 μM

flecainide at diastolic [Ca^{2+}]. The [flecainide]-dependent reduction in burst duration reported

here and previously (Hilliard et al., 2010) indicates another, faster mechanism of inhibition

that might be an increased deactivation rate of the RyR2 channel caused by flecainide (*i.e.* the

deactivation transition in Figure 10).

The anaesthetics, procaine and the quaternary amine derivatives of lidocaine (QX314,

QX222) have been shown to act on RyR2 only when applied to the cytoplasmic side of the

membrane (Tinker and Williams, 1993; Xu et al., 1993). However, determination of the side

of the membrane from which flecainide binds to the RyR2 is complicated by the fact that

flecainide is membrane permeable. For example, in cardiomyocytes, flecainide must enter the

cell to reach its site of action on Nav1.5 channels (Strichartz, 1973; Wang et al., 1995). In our

bilayer experiments, flecainide when applied to either side of the membrane exhibited the

same voltage-dependent modes of block suggesting that flecainide readily crosses the bilayer

and that cytoplasmic and luminal flecainide act by a common mechanism. The 3-fold lower

potency for flecainide on the luminal side (relative to cytoplasmic) and the fact that flecainide

inhibition was only sensitive to cytoplasmic pH indicates that the flecainide site of action is

only accessible from the cytoplasmic solution.

We observed distinctly different [Cs^+]- and voltage-dependencies of the flecainide on- and

off-rates associated with fast and slow block (Figures 8 and 9) suggesting that the fast and

slow modes operate via different binding sites. However, the mechanisms for the [Cs^+]- and

voltage-dependencies are not yet clear. The Woodhull model (Woodhull, 1973) does not

readily explain the non-exponential voltage-dependence of rate constant for the fast mode of

block (Figure 8B). An alternative model has been proposed to explain the voltage-

dependence of binding of uncharged drugs to RyR2 such as amitryptyline and ryanodols (Chopra et al., 2009; Tanna et al., 2000). In that model, the voltage-dependence of energy barrier profiles is due to distortion of the binding site by the electric field. It is possible that both mechanisms contribute to the observed voltage-dependence of flecainide block.

The fast RyR2 blocking mode of flecainide appears to be a common property of local anaesthetics. Cocaine (Tsushima et al., 1996), quinidine, quinadinium (Tsushima et al., 2002) and the quaternary amine derivative of lidocaine (QX314, (Xu et al., 1993)) inhibit RyR2 with a flicker block comprising a conductance substate and complete channel closures. The voltage-dependence of fast flecainide inhibition has an effective valency (δ) of 1.4, which is similar to that reported for quinidine (1.2, (Tsushima et al., 2002)) and QX314 (1.4, (Tinker et al., 1992)). These voltage-dependencies were seen as evidence that the local anaesthetics bind in the channel pore. However, the strongest evidence for this comes from mutagenesis studies in Na^+ and K^+ that show amino acid residues near the cytoplasmic end of the pore channels are important for binding of local anaesthetics including flecainide (Ragsdale et al., 1994; Ragsdale et al., 1996; Yeola et al., 1996). The slow block of RyR2 has also been reported for tetracaine (Laver and van Helden, 2011; Xu et al., 1993) and that also was seen to be a closed stated blocking mechanism.

In Nav1.5 channels, three local anaesthetic blocking mechanisms have been identified (Sheets et al., 2010): 1) an open/inactivated state block associated with a reduction in the gating charge and stabilisation of the S4 segments, 2) a resting closed state block that may involve a diffuse binding region in the inner vestibule of the pore, and 3) a fast flicker block due to interaction of the charged forms of local anaesthetics with the cytoplasmic side of the selectivity filter. The slow and fast modes for flecainide block of RyR2 have similar characteristics as the latter two forms of Na^+ channel block (items 2 & 3, respectively).

Under systolic conditions, tetracaine shares very similar RyR2 inhibition mechanisms with flecainide (Laver and van Helden, 2011). They both have fast and slow modes of block where only the slow mode has a preference for the closed RyR2 confirmation. This raises a question as to why drugs with such similar mechanisms of action have such different effects on Ca^{2+} release events. Flecainide increases Ca^{2+} spark frequency but reduces their amplitude whereas tetracaine only reduces spark frequency. Moreover, flecainide reduces the occurrence of Ca^{2+} waves while tetracaine increases Ca^{2+} wave amplitude (Hilliard et al., 2010). The answer may lie in the relative off-rates of flecainide and tetracaine associated with their slow modes of block. It has been proposed that tetracaine destabilizes SR Ca^{2+} release because it is a more potent inhibitor of Ca^{2+} release during diastole. This would increase diastolic Ca^{2+} loading of the SR leading to an increase in systolic Ca^{2+} release when tetracaine block is alleviated (Laver and van Helden, 2011). During the course of the heartbeat, the relatively fast off-rate of tetracaine (~20 s^{-1}) will allow substantial loss in its blocking potency during systole. This would effectively increase the feedback on SR Ca^{2+} release generated by cytoplasmic and luminal Ca^{2+} and promote instability of Ca^{2+} release. Whereas the slower off-rate for flecainide (~1 s^{-1}) will tend to sustain flecainide block throughout systole.

The better anti-arrhythmic efficacy of flecainide versus tetracaine may lie in its different blocking kinetics under diastolic conditions. Flecainide reduces burst duration of RyR2 activity at diastolic cytoplasmic [Ca^{2+}] whereas tetracaine does not (Hilliard et al., 2010). However, it needs to be emphasized that, in addition to RyR2 inhibition, Na^+ channel block by flecainide is clearly important for its efficacy in CPVT. Reducing the Na^+ current can 1) inhibit action potentials triggered by NCX-mediated depolarisations (Watanabe et al., 2009) and 2) increase NCX-mediated Ca^{2+} efflux leading to a decrease in Ca^{2+} concentration in the vicinity of RyR2 (Sikkel et al., 2013; Steele et al., 2013).

In conclusion, we find that in systolic $[Ca^{2+}]$, flecainide causes RyR2 closures via independent fast and slow modes. The slow mode has a preference for the closed RyR2 confirmation whereas the fast mode does not depend on RyR2 state. Flecainide accesses its sites of action for both modes of inhibition from the cytoplasmic side of the membrane. In diastolic $[Ca^{2+}]$, there is another flecainide inhibition mechanism causing an open channel block, in addition for the fast and slow modes.

AKNOWLEDGEMENTS

AUTHORSHIP CONTRIBUTIONS

Participated in research design: Mehra, Laver

Conducted experiments: Mehra,

Contributed new reagents or analytic tools: Laver

Performed data analysis: Mehra, Laver

Wrote or contributed to the writing of the manuscript: Knollmann, Mehra, Imtiaz, vanHelden,

Laver

REFERENCES

Anno T and Hondeghem LM (1990) Interactions of flecainide with guinea pig cardiac sodium channels. Importance of activation unblocking to the voltage dependence of recovery. *Circulation research* **66**(3):789-803.

Blayney LM and Lai FA (2009) Ryanodine receptor-mediated arrhythmias and sudden cardiac death. *Pharmacol Ther* **123**(2):151-177.

Borchard U and Boisten M (1982) Effect of flecainide on action potentials and alternating current-induced arrhythmias in mammalian myocardium. *Journal of cardiovascular pharmacology* **4**(2):205-212.

Campbell TJ and Vaughan Williams EM (1983) Voltage- and time-dependent depression of maximum rate of depolarisation of guinea-pig ventricular action potentials by two new antiarrhythmic drugs, flecainide and lorcainide. *Cardiovascular research* **17**(5):251-258.

Cannell MB and Soeller C (1997) Numerical analysis of ryanodine receptor activation by L-type channel activity in the cardiac muscle dyad. *Biophysical journal* **73**(1):112-122.

Chopra N, Laver D, Davies SS and Knollmann BC (2009) Amitriptyline activates cardiac ryanodine channels and causes spontaneous sarcoplasmic reticulum calcium release. *Mol Pharmacol* **75**(1):183-195.

Chung SH, Moore JB, Xia LG, Premkumar LS and Gage PW (1990) Characterization of single channel currents using digital signal processing techniques based on Hidden Markov Models. *Philos Trans R Soc Lond Biol* **329**:265-285.

Dibb KM, Eisner DA and Trafford AW (2007) Regulation of systolic $[Ca^{2+}]_i$ and cellular Ca^{2+} flux balance in rat ventricular myocytes by SR Ca^{2+}, L-type Ca^{2+} current and diastolic $[Ca^{2+}]_i$ *The Journal of physiology* **585**(Pt 2):579-592.

George CH, Higgs GV and Lai FA (2003) Ryanodine receptor mutations associated with stress-induced ventricular tachycardia mediate increased calcium release in stimulated cardiomyocytes. *Circ Res* **93**(6):531-540.

Grant AO, Chandra R, Keller C, Carboni M and Starmer CF (2000) Block of wild-type and inactivation-deficient cardiac sodium channels IFM/QQQ stably expressed in mammalian cells. *Biophysical journal* **79**(6):3019-3035.

Hilliard FA, Steele DS, Laver D, Yang Z, Le Marchand SJ, Chopra N, Piston DW, Huke S and Knollmann BC (2010) Flecainide inhibits arrhythmogenic Ca^{2+} waves by open state block of ryanodine receptor Ca^{2+} release channels and reduction of Ca^{2+} spark mass, in *Journal of molecular and cellular cardiology* pp 293-301.

Knollmann BC, Chopra N, Hlaing T, Akin B, Yang T, Ettensohn K, Knollmann BE, Horton KD, Weissman NJ, Holinstat I, Zhang W, Roden DM, Jones LR, Franzini-Armstrong C and Pfeifer K (2006a) Casq2 deletion causes sarcoplasmic reticulum volume increase, premature Ca2+ release, and catecholaminergic polymorphic ventricular tachycardia. *J Clin Invest* **116**(9):2510-2520.

Knollmann BC, Chopra N, Hlaing T, Akin B, Yang T, Ettensohn K, Knollmann BE, Horton KD, Weissman NJ, Holinstat I, Zhang W, Roden DM, Jones LR, Franzini-Armstrong C and Pfeifer K (2006b) Casq2 deletion causes sarcoplasmic reticulum volume increase, premature Ca^{2+} release, and catecholaminergic polymorphic ventricular tachycardia. *J Clin Invest* **116**(9):2510-2520.

Kojima M, Hamamoto T and Ban T (1989) Sodium channel-blocking properties of flecainide, a class IC antiarrhythmic drug, in guinea-pig papillary muscles. An open channel blocker or an inactivated channel blocker. *Naunyn-Schmiedeberg's archives of pharmacology* **339**(4):441-447.

Laver DR, O'Neill ER and Lamb GD (2004) Luminal Ca^{2+}-regulated Mg^{2+} inhibition of skeletal RyRs reconstituted as isolated channels or coupled clusters. *J Gen Physiol* **124**(6):741-758.

Laver DR, Roden LD, Ahern GP, Eager KR, Junankar PR and Dulhunty AF (1995) Cytoplasmic Ca^{2+} inhibits the ryanodine receptor from cardiac muscle. *JMembrBiol* **147**(1):7-22.

Laver DR and van Helden DF (2011) Three independent mechanisms contribute to tetracaine inhibition of cardiac calcium release channels. *Journal of molecular and cellular cardiology* **51**(3):357-369.

Liu H, Atkins J and Kass RS (2003) Common molecular determinants of flecainide and lidocaine block of heart Na^+ channels: evidence from experiments with neutral and quaternary flecainide analogues. *The Journal of general physiology* **121**(3):199-214.

Liu H, Tateyama M, Clancy CE, Abriel H and Kass RS (2002) Channel openings are necessary but not sufficient for use-dependent block of cardiac Na^+ channels by flecainide: evidence from the analysis of disease-linked mutations. *The Journal of general physiology* **120**(1):39-51.

Liu N, Colombi B, Memmi M, Zissimopoulos S, Rizzi N, Negri S, Imbriani M, Napolitano C, Lai FA and Priori SG (2006) Arrhythmogenesis in catecholaminergic polymorphic ventricular tachycardia: insights from a RyR2 R4496C knock-in mouse model. *Circulation research* **99**(3):292-298.

McCauley MD and Wehrens XH (2011) Targeting ryanodine receptors for anti-arrhythmic therapy. *Acta Pharmacol Sin* **32**(6):749-757.

Nabauer M, Ellis-Davies GC, Kaplan JH and Morad M (1989) Modulation of Ca^{2+} channel selectivity and cardiac contraction by photorelease of Ca^{2+}. *Am J Physiol* **256**(3 Pt 2):H916-920.

Nagatomo T, January CT and Makielski JC (2000) Preferential block of late sodium current in the LQT3 DeltaKPQ mutant by the class I(C) antiarrhythmic flecainide. *Molecular pharmacology* **57**(1):101-107.

Nitta J, Sunami A, Marumo F and Hiraoka M (1992) States and sites of actions of flecainide on guinea-pig cardiac sodium channels. *European journal of pharmacology* **214**:191-197.

Nyegaard M, Overgaard MT, Sondergaard MT, Vranas M, Behr ER, Hildebrandt LL, Lund J, Hedley PL, Camm AJ, Wettrell G, Fosdal I, Christiansen M and Borglum AD (2012) Mutations in calmodulin cause ventricular tachycardia and sudden cardiac death. *American journal of human genetics* **91**(4):703-712.

O'Neill ER, Sakowska MM and Laver DR (2003) Regulation of the Calcium Release Channel from Skeletal Muscle by Suramin and the Disulfonated Stilbene Derivatives DIDS, DBDS, and DNDS. *BiophysJ* **84**(3):1674-1689.

Postma AV, Denjoy I, Hoorntje TM, Lupoglazoff JM, Da Costa A, Sebillon P, Mannens MM, Wilde AA and Guicheney P (2002) Absence of calsequestrin 2 causes severe forms of catecholaminergic polymorphic ventricular tachycardia. *Circulation research* **91**(8):e21-e26.

Priori SG, Napolitano C, Tiso N, Memmi M, Vignati G, Bloise R, Sorrentino VV and Danieli GA (2001) Mutations in the Cardiac Ryanodine Receptor Gene (hRyR2) Underlie Catecholaminergic Polymorphic Ventricular Tachycardia. *Circulation* **103**(2):196-200.

Ragsdale DS, McPhee JC, Scheuer T and Catterall WA (1994) Molecular determinants of state-dependent block of Na^+ channels by local anesthetics. *Science* **265**(5179):1724-1728.

Ragsdale DS, McPhee JC, Scheuer T and Catterall WA (1996) Common molecular determinants of local anesthetic, antiarrhythmic, and anticonvulsant block of voltage-gated Na$^+$ channels. *Proceedings of the National Academy of Sciences of the United States of America* **93**(17):9270-9275.

Sheets MF, Fozzard HA, Lipkind GM and Hanck DA (2010) Sodium channel molecular conformations and antiarrhythmic drug affinity. *Trends in cardiovascular medicine* **20**(1):16-21.

Sigworth FJ and Sine SM (1987) Data transformations for improved display and fitting of single- channel dwell time histograms. *BiophysJ* **52**:1047-1054.

Sikkel MB, Collins TP, Rowlands C, Shah M, O'Gara P, Williams AJ, Harding SE, Lyon AR and MacLeod KT (2013) Flecainide reduces Ca(2+) spark and wave frequency via inhibition of the sarcolemmal sodium current. *Cardiovasc Res* **98**(2):286-296.

Steele DS, Hwang HS and Knollmann BC (2013) Triple mode of action of flecainide in catecholaminergic polymorphic ventricular tachycardia. *Cardiovasc Res* **98**(2):326-327.

Strichartz GR (1973) The inhibition of sodium currents in myelinated nerve by quaternary derivatives of lidocaine. *The Journal of general physiology* **62**(1):37-57.

Tanna B, Welch W, Ruest L, Sutko JL and Williams AJ (2000) The interaction of a neutral ryanoid with the ryanodine receptor channel provides insights into the mechanisms by which ryanoid binding is modulated by voltage. *J Gen Physiol* **116**(1):1-9.

Tinker A, Lindsay AR and Williams AJ (1992) Large tetraalkyl ammonium cations produce a reduced conductance state in the sheep cardiac sarcoplasmic reticulum Ca^{2+}-release channel. *Biophysical journal* **61**(5):1122-1132.

Tinker A and Williams AJ (1993) Charged local anesthetics block ionic conduction in the sheep cardiac sarcoplasmic reticulum calcium release channel. *Biophys J* **65**:852-864.

Tsushima RG, Kelly JE and Wasserstrom JA (1996) Characteristics of cocaine block of purified cardiac sarcoplasmic reticulum calcium release channels. *Biophysical journal* **70**(3):1263-1274.

Tsushima RG, Kelly JE and Wasserstrom JA (2002) Subconductance activity induced by quinidine and quinidinium in purified cardiac sarcoplasmic reticulum calcium release channels. *The Journal of pharmacology and experimental therapeutics* **301**(2):729-737.

Wang Z, Fermini B and Nattel S (1995) Effects of flecainide, quinidine, and 4-aminopyridine on transient outward and ultrarapid delayed rectifier currents in human atrial myocytes. *The Journal of pharmacology and experimental therapeutics* **272**(1):184-196.

Watanabe H, Chopra N, Laver D, Hwang HS, Davies SS, Roach DE, Duff HJ, Roden DM, Wilde AA and Knollmann BC (2009) Flecainide prevents catecholaminergic polymorphic ventricular tachycardia in mice and humans. *Nat Med* **15**(4):380-383.

Watanabe H and Knollmann BC (2011) Mechanism underlying catecholaminergic polymorphic ventricular tachycardia and approaches to therapy. *J Electrocardiol*.

Woodhull AM (1973) Ionic blockage of sodium channels in nerve. *J Gen Physiol* **61**(687):708.

Xu L, Jones R and Meissner G (1993) Effects of local anesthetics on single channel behavior of skeletal muscle calcium release channel. *The Journal of general physiology* **101**(2):207-233.

Yeola SW, Rich TC, Uebele VN, Tamkun MM and Snyders DJ (1996) Molecular analysis of a binding site for quinidine in a human cardiac delayed rectifier K$^+$ channel. Role of S6 in antiarrhythmic drug binding. *Circulation research* **78**(6):1105-1114.

Zhou Q, Xiao J, Jiang D, Wang R, Vembaiyan K, Wang A, Smith CD, Xie C, Chen W, Zhang J, Tian X, Jones PP, Zhong X, Guo A, Chen H, Zhang L, Zhu W, Yang D, Li X, Chen J, Gillis AM, Duff HJ, Cheng H, Feldman AM, Song LS, Fill M, Back TG and Chen SR (2011) Carvedilol and its new analogs suppress arrhythmogenic store overload-induced Ca2+ release. *Nat Med* **17**(8):1003-1009.

FIGURE CAPTIONS

Figure 1. Flecainide inhibition of RyR2 open probability under various experimental conditions. Representative single channel recordings of sheep RyR2 at +40 mV showing of inhibition by flecainide in the cytoplasmic **(A)** and luminal **(B)** bath. ([Flecainide] at the end of each trace). The cytoplasmic bath contained 2 mM ATP, free Ca^{2+} = 0.1 mM and free Mg^{2+} = 1 mM. The luminal bath contained 0.1 mM Ca^{2+}. Channel openings appear as upward current jumps from the baseline (top traces, the channel closed state indicated by dashed line). **(C)** [Flecainide]-dependencies of RyR2 open probability (P_o) relative to that in the absence of flecainide (experimental conditions, legend and n values given in Table 1.) **(D)** The voltage-dependence of IC_{50} for cytoplasmic and luminal flecainide inhibition (symbols in Table 1).

Figure 2. Fast and slow modes of flecainide block in systolic $[Ca^{2+}]$ and $[Mg^{2+}]$. (A, B) Representative single channel recordings of RyR2 at +40 mV showing inhibition by cytoplasmic flecainide in the presence of various cytoplasmic $[Mg^{2+}]$ and $[Ca^{2+}]$ (concentrations at the left of each trace). Channel openings appear as upward current jumps from the baseline. **(C, D)** Closed dwell-time histograms showing the rate of closed events based on the method of Sigworth and Sine (1987) as described in the text. Histograms were compiled from 60 s recordings from which the traces in A and B were taken. The data (O) is fitted with three exponential decays with time constants τ_F, τ_S and $\tau_{Mg/Ca}$, the latter arising from closures associated with Mg^{2+}/Ca^{2+} inhibition of RyR2. τ_F and τ_S appear as peaks in these plots indicated by the arrows. $\tau_{Mg/Ca}$ is poorly resolved and appears as a shoulder near τ_F. (●) is fitted with two exponential decays with time constants τ_F, τ_S where the latter is a relatively small peak. **(E)** Corresponding open dwell-time histograms for the top and bottom traces in (A). **(F)** Dependencies of mean open time, τ_o, on flecainide concentration (n = 3-9).

Figure 3. Fast and slow modes of flecainide block in diastolic [Ca^{2+}]. (A, B) Representative single channel recordings of RyR2 at +40 mV showing inhibition by cytoplasmic flecainide in the presence of 0.1 μM Ca^{2+} (A) or 0.1 μM Ca^{2+} plus 5 mM caffeine (B). Channel openings appear as upward current jumps from the baseline. **(C, D)** Closed dwell-time histograms compiled 60 s recordings from which the traces in A and B were taken. The data are fitted with two exponential decays with time constants τ_F and τ_S that appear as peaks in these plots indicated by the arrows. **(E, F)** Concentration dependencies of the mean duration of long flecainide induced (τ_S) closures and mean open time (τ_o) in the present an absence of 5 mM caffeine. The dashed line represents values obtained in the presence of 100 μM cytoplasmic Ca^{2+} plus 1 mM Mg^{2+}. The legend in F applies to E. * indicates significant difference from zero flecainide (p < 0.05).

Figure 4. Rates of slow (A) and fast modes (B) of flecainide block associated with the illustrated reaction schemes. Block was induced by 50 μM flecainide in the presence of various cytoplasmic concentrations of caffeine, Ca^{2+} and Mg^{2+}. The fast mode on-rate, $R_{Fon} = 1/\tau_o$ and $R_{Foff} = 1/\tau_F$. The slow mode on-rate, R_{Son} equals the inverse of the time between long closures (defined here as closures longer than 200 ms) and R_{Soff} equals the inverse of τ_S. Note that slow mode inhibition was not resolved in 0.1 μM Ca^{2+} alone. Asterisks indicate significant differences from 0.1 μM Ca^{2+} plus caffeine in A and 0.1 μM Ca^{2+} alone in B (* p<0.05, ** p<0.01).

Figure 5. The slow mode of flecainide block is a closed channel block as described by the scheme in (A). In the reaction scheme, the dashed rectangle encloses open and closed states of the RyR2 that appear as bursts of activity between slow-mode blocking events (defined here as closures > 200 ms). According to this scheme, R_{Son} increases with RyR2 closed

probability and with [flecainide]. **(B)** The on-rate R_{Son} increases with RyR2 closed probability

within bursts regardless of cytosolic $[Ca^{2+}]$ and $[Mg^{2+}]$ or the presence of caffeine. **(C)** The

on-rate R_{Son} increases proportionally with [flecainide] (proportionality indicated by the

dashed line). **(D)** Confirms that the rate constants for slow flecainide block (see equations in

A) do not depend on cytosolic $[Mg^{2+}]$.

Figure 6. The flecainide cation is a more potent blocker than its neutral form.
Cytoplasmic flecainide (pKa = 9.2) at 50μM causes flicker block of RyR2 at pH 7.4. **(A, B)**
Recordings obtained at +40 mV with cytoplasmic conditions as indicated. As the pH was

raised to pH 9.5 in the presence of flecainide, the block was abolished within the time of

solution exchange. Channel openings appear as upward current jumps from the baseline. (A)

Shows alleviation of fast block at high pH and (B) where 1 mM Mg^{2+} is present, shows

alleviation of fast and slow block at high pH. **(C, D)** Closed time histograms compiled form

the records in B indicating the time constants for fast and slow inhibition τ_F and τ_S,

respectively. pH 9.5 attenuates the peak associated with slow inhibition. **(E-G)** Rate constants

for fast and slow inhibition modes and their dependence on cytoplasmic and luminal pH. Rate

constants were derived from histograms as described in the text. Asterisks indicate significant

differences from pH 7.4 in both *cis* and *trans* solutions (* p<0.05, ** p<0.01).

Figure 7. Substate analysis of fast-mode block of RyR2. (A) Representative single channel

recordings of RyR2 at +60 mV. The cytoplasmic bath contained 2 mM ATP and 1 mM CaCl₂

(free Ca^{2+} = 0.45 mM) and luminal bath contained 0.1 mM Ca^{2+}. Addition of flecainide

(cytoplasmic concentrations at the left of each trace) resulted in more frequent channel

closures and appearance of substates at ~25% of the maximum conductance. **(B)** Current-

voltage relationships for maximum and substates in the presence of 50 μM flecainide (n=8-

16). **(C)** Model for fast mode block. According to this model, the on-rates, R_{OS} and R_{SC}, are proportional to [flecainide] and the off-rates, R_{SO} and R_{CS}, are independent of [flecainide]. **(D)** The on-rates are proportional to [flecainide] and the off-rates are independent of [flecainide]. Transition rates were derived from HMM analysis (n=3). Symbols show the mean ± S.E.M.

Figure 8. Voltage-dependencies of rate constants for slow (A) and fast modes of block (B). (A) Slow mode rate constants were calculated as described in Figure 5A (n = 5-10). **(B)** Fast mode rate constants were calculated as described in Figure 7C (n=3-5). Where no error bars are visible they are contained within the symbol.

Figure 9. Cytosolic [Cs$^+$]-dependence of the rate constants for flecainide inhibition by slow and fast modes (+40mV). The slow mode of block was measured at in the presence of cytoplasmic 1 mM Mg^{2+}, 2 mM ATP and 100 μM Ca^{2+}. The fast mode was measured in the absence of Mg^{2+}. ** indicates significant difference (p<0.01).

Figure 10. Overall scheme showing the various mechanisms proposed here for flecainide inhibition of RyR2. Asterisks indicate reaction steps that depend on flecainide.

TABLE 1

Symbol (Fig 1C & D)	Side of flecainide addition	Cytoplasmic ion concs. Cs^+ mM	Ca^{2+} μM	Mg^{2+} mM	IC_{50} μM	H	$P_o\ max$	n
○	cis	250	100	0	87 ± 6	1.2 ± 0.2	0.97 ± 0.02	6
●	trans	250	100	0	250 ± 50	0.6 ± 0.2	0.91 ± 0.02	3
△	cis	250	100	1	25 ± 4	1.0 ± 0.3	0.75 ± 0.06	5
◇	cis	150	100	1	5.0 ± 1.0	1.4 ± 0.8	0.37 ± 0.10	4
□	cis	250	0.1	0	17 ± 2	2.0 ± 1.0	0.055 ± 0.038	8

Table 1. Flecainide concentrations for half inhibition of RyR2 (IC_{50}), Hill coefficients (H), open probability in the absence of flecianide ($P_o\ max$) and numbers of experiments (n) under various experimental conditions obtained from the dose-response curves in Figure 1C. In each case, the luminal solution contained 250 mM Cs^+, 100 μM Ca^{2+} and no Mg^{2+}.

A cytoplasmic flecainide, +40 mV

[cyt]

0 μM

10 μM

20 μM

50 μM

100 μM

B luminal flecainide, +40 mV

[lum]

0 μM

300 μM

500 μM

700 μM

15 pA ⌐ 5s

C +40 mV

relative P_o

[flecainide], μM

D

IC_{50}
μM

membrane potential, mV
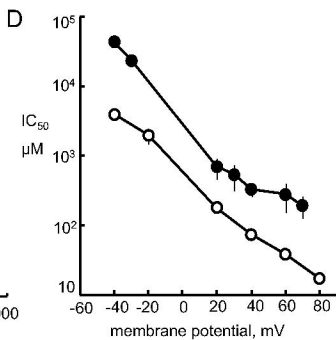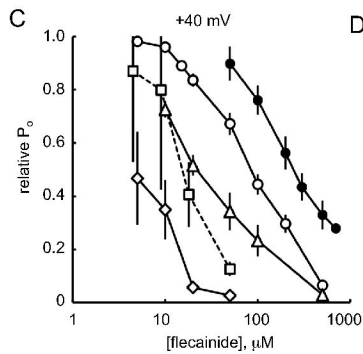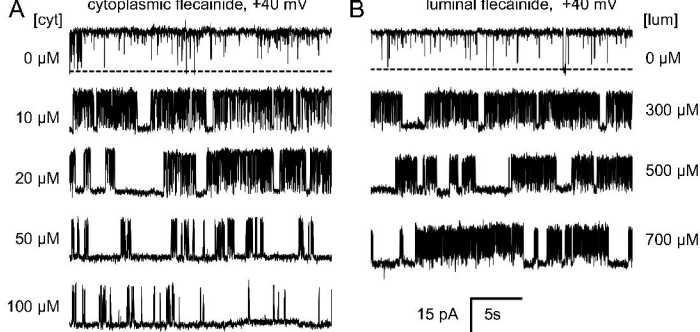
Figure 1

Figure 2

Figure 3

Figure 4

Figure 5

Figure 6

A

+60 mV

[cyt]

0 μM ← Open, ← Closed

40 μM ← Open, ← Substate

100 μM ← Open, ← Substate

500 μM ← Open, ← Substate

20 pA | 20 ms

B

I, pA

Substate - ○
Open state   (0 μM) - ▲
Open state (50 μM) - △

C

$$\text{Open} \underset{k_{so}}{\overset{k_{os}}{\rightleftharpoons}} \begin{array}{c}\text{Substate}\\(1 \text{ flec})\end{array} \underset{k_{cs}}{\overset{k_{sc}}{\rightleftharpoons}} \begin{array}{c}\text{Closed}\\(2 \text{ flec})\end{array}$$

$$R_{os} = k_{os} \times [\text{flecainide}]$$

$$R_{sc} = k_{sc} \times [\text{flecainide}]$$

$$R_{so} = k_{so} \qquad R_{cs} = k_{cs}$$

D

R_{os} - ● R_{sc} - ▲
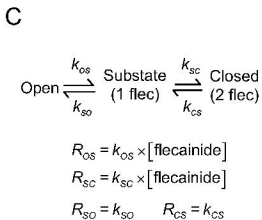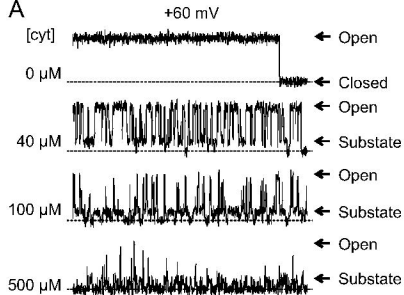R_{so} - ○ R_{cs} - △

+60 mV

transition rate (ms⁻¹)
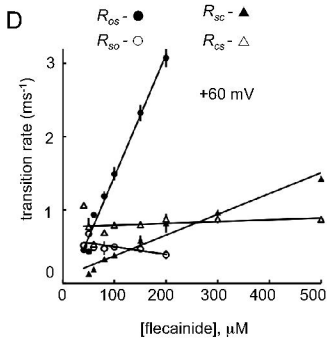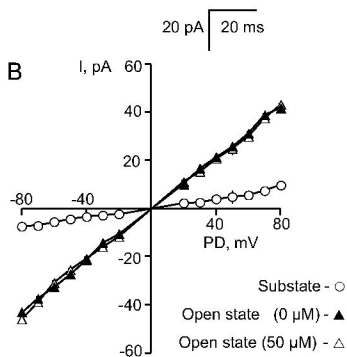
[flecainide], μM

Figure 7

Figure 8

Figure 9

Closed $\rightleftharpoons$ Substate $\rightleftharpoons$ Open $\overset{*}{\rightleftharpoons}$ Closed $\overset{*}{\rightleftharpoons}$ Closed

fast mode fast mode RyR2 activated RyR2 deactivated slow mode
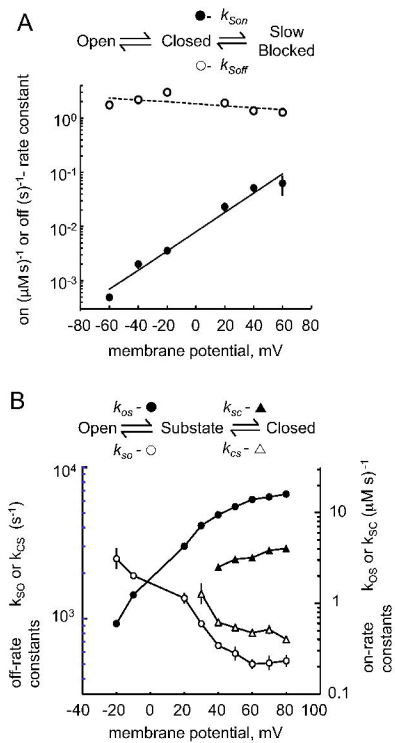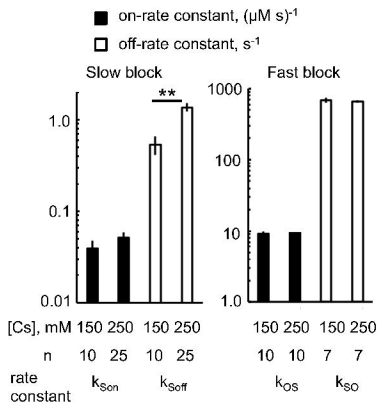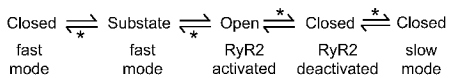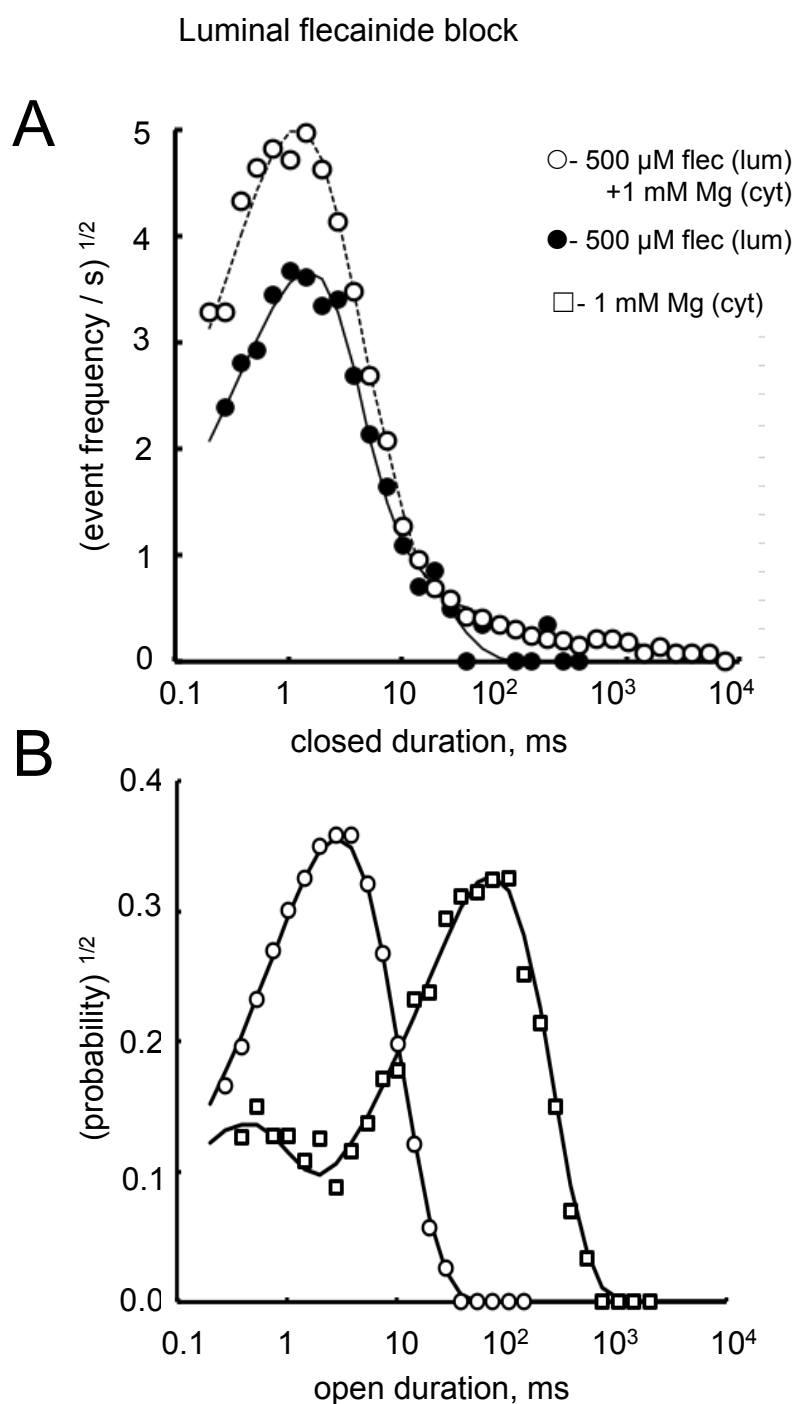
Figure 10

Multiple modes of RyR2 inhibition by flecainide

D. Mehra, M.S. Imtiaz, D.F. van Helden, B.C. Knollmann and D.R. Laver

Moleclar Pharmacology

Luminal flecainide block

Supplemental Figure. Dwell-time analysis of luminal flecainide inhibition. (A) Closed dwell-time histograms showing the rate of closed events based on the method of Sigworth and Sine (1987) as described in the text. **(B)** Corresponding open dwell-time histograms. The legend applies to A and B.